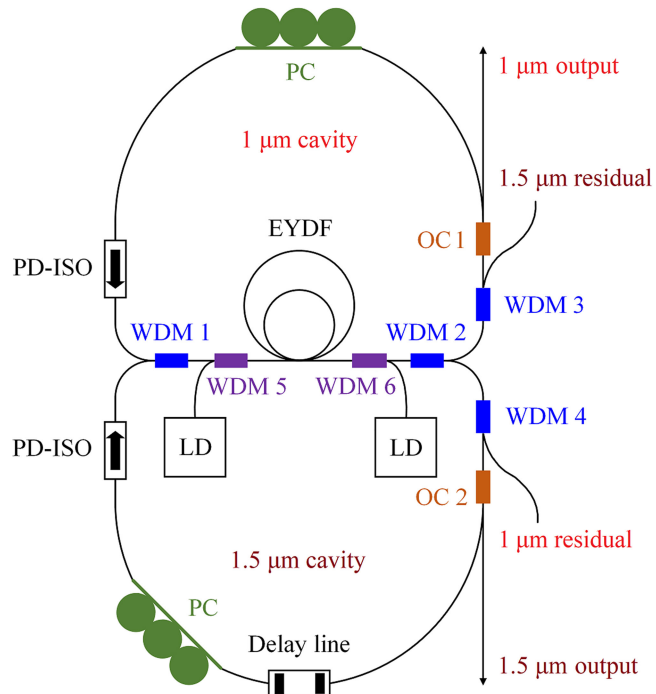


# 1/1.5 $\mu\text{m}$ Synchronized Dual-Band Mode-Locked Fiber Laser

Volume 13, Number 1, February 2021

Chunyu Guo  
Shupeng Lian  
Shuangchen Ruan  
Xiaogang Ge  
Peiguang Yan  
Jiachen Wang  
Ping Hua  
Qitao Lue



DOI: 10.1109/JPHOT.2020.3046761

# 1/1.5 $\mu\text{m}$ Synchronized Dual-Band Mode-Locked Fiber Laser

Chunyu Guo<sup>1</sup>, Shupeng Lian,<sup>1</sup> Shuangchen Ruan,<sup>1,2</sup>  
Xiaogang Ge,<sup>1</sup> Peiguang Yan<sup>1</sup>, Jiachen Wang<sup>1</sup>, Ping Hua,<sup>3</sup>  
and Qitao Lue<sup>4</sup>

<sup>1</sup>Shenzhen Key Laboratory of Laser Engineering, Key Laboratory of Advanced Optical Precision Manufacturing Technology of Guangdong Higher Education Institutes, Guangdong Provincial Key Laboratory of Micro/Nano Optomechatronics Engineering, College of Physics and Optoelectronic Engineering, Shenzhen University, Shenzhen 518060, China

<sup>2</sup>College of New Materials and New Energies, Shenzhen Technology University, Shenzhen 518118, China

<sup>3</sup>Faculty of Engineering and Physical Sciences, University of Southampton, Southampton SO171BJ, U.K.

<sup>4</sup>Han's Laser Technology Industry Group Company, Ltd., Shenzhen 518057, China

DOI:10.1109/JPHOT.2020.3046761

This work is licensed under a Creative Commons Attribution-NonCommercial-NoDerivatives 4.0 License. For more information, see <https://creativecommons.org/licenses/by-nc-nd/4.0/>

Manuscript received November 11, 2020; revised December 13, 2020; accepted December 20, 2020. Date of publication December 23, 2020; date of current version January 7, 2021. This work was supported in part by the National Natural Science Foundation of China (NSFC) under Grants 61975136, 61935014, 61775146, and 61905151, in part by the Outstanding Young Teacher Cultivation Projects in Guangdong Province YQ2015142, in part by the Guangdong Basic and Applied Basic Research Foundation under Grant 2019A1515010699, and in part by the Shenzhen Science and Technology Project under Grants JCYJ20180305125352956, JCYJ20160520161351540, JCYJ20170817100639177, JCYJ20170302151146995 and JCYJ20160328144942069. Corresponding author: Jiachen Wang (e-mail: Alphafirefox@gmail.com).

**Abstract:** A 1/1.5  $\mu\text{m}$  dual-band mode-locked fiber laser is experimentally demonstrated. The laser is based upon an architecture in which the 1  $\mu\text{m}$  and the 1.5  $\mu\text{m}$  signals are generated in independent cavities that share the identical active fiber. The mode-locking of the 1  $\mu\text{m}$  laser is realized via nonlinear polarization evolution (NPE), whilst the 1.5  $\mu\text{m}$  laser is mode-locked through cross-phase modulation (XPM) induced by the 1  $\mu\text{m}$  laser and the mode-locking is further stabilized by NPE. Synchronized dual-band mode-locking operation is achieved using the laser.

**Index Terms:** Fiber lasers, Dual-wavelength lasers, Mode-locked lasers.

## 1. Introduction

Mode-locked fiber lasers are powerful tools in a range of industrial and scientific applications, such as supercontinuum generation, sensing, material processing, spectroscopy, and medical surgery [1]. In recent years, there is a growing interest in the so-called dual-band mode-locked fiber lasers in which the optical pulses are generated in two distinct spectral bands simultaneously. Unlike conventional dual-wavelength lasers [2]–[5] which operate at two adjacent wavelengths (i.e., the two lasing wavelengths are within the identical spectral band), dual-band lasers generate radiations at two wavelengths locating far apart (e.g., 1/1.5  $\mu\text{m}$ , 1.5/2  $\mu\text{m}$ , etc.). Such lasers exhibit unique advantages in the applications where radiations from different spectral bands are required simultaneously. For example, dual-band pulsed lasers are useful in multi-color pump-probe systems, Raman spectroscopy, nonlinear frequency conversion systems such as difference frequency

generation (DFG), ultrabroadband supercontinuum generation, or to develop transmitters working simultaneously in two optical communication windows [6]–[9]. The development of such systems is challenging, in view of that the dual-band operation usually requires two gain regions (i.e., active fibers) and thus, complex laser configuration is anticipated.

In order to optimize the performance, synchronization between the two-color pulses is desired for dual-band mode-locked laser systems. Thus far, the research efforts on synchronized dual-band mode-locking are still not abundant. In the past decades several active, passive, and active/passive hybrid mechanisms have been developed for realizing synchronized two-color pulses in solid-state laser systems [10]–[13], and these mechanisms can be similarly applied on fiberized systems. A representative approach to achieve synchronized dual-band mode-locking in fiber laser systems is to employ a single saturable absorber for establishing the mode-locking of the two-color pulses, and the synchronization between the two-color pulses is facilitated by nonlinear effects such as XPM [8], [14].

At present, most reported dual-band mode-locked laser systems adopt architectures that comprise two independent gain regions (e.g., active fibers). This can be attributed to the fact that a two-color source which relies on a single gain medium usually suffers from limited bandwidths and strong gain competition. In this paper, we experimentally demonstrate a 1/1.5  $\mu\text{m}$  dual-band mode-locked fiber laser that operates with synchronization between the 1/1.5  $\mu\text{m}$  pulses. The laser, featuring a “figure- $\theta$ ” configuration, generates the two-color pulses from a single active fiber. The 1  $\mu\text{m}$  laser is mode-locked via conventional NPE. The generated 1  $\mu\text{m}$  pulse subsequently mode-locks the 1.5  $\mu\text{m}$  laser through XPM. For enhancing the stability, the mode-locking of the 1.5  $\mu\text{m}$  laser is further assisted by NPE. The XPM-induced mode-locking requires a strict match between the cavity length of the 1.5  $\mu\text{m}$  laser and the repetition rate of the 1  $\mu\text{m}$  laser, and once the match is reached the system is capable of realizing synchronized dual-band mode-locking. In this work, by precisely matching the cavity length and the repetition rate, picosecond two-color pulses are generated using the system with a common repetition rate of 25.89 MHz. Restricted by the maximum available pump power, the highest energies of the 1  $\mu\text{m}$  and 1.5  $\mu\text{m}$  pulse achieved in this work are respectively 1.06 nJ and 0.11 nJ. The generated dual-band pulses are synchronized, and they are extracted from the laser cavity through different output ports for independent usage. The laser exhibits superiority over previously reported systems in compactness and cost-effectiveness, given that it uses a single active fiber.

## 2. Experimental Setup

The diagram of the experimental setup is presented in Fig. 1. The system is of a “figure- $\theta$ ” architecture. The 1  $\mu\text{m}$  laser and the 1.5  $\mu\text{m}$  laser each have their own ring cavities, and the two cavities are attached together by a shared section that comprises the active fiber. The active fiber is 1.7 m Er/Yb-codoped fiber (CorActive EY305, single clad fiber), which is pumped by a pair of 976 nm laser diodes (Oclaro LC962UA74P-20R) from both directions. The pump radiation is injected into the active fiber through 980/1064&1550 nm WDMs. Two 1064/1550 nm WDMs separate the “figure- $\theta$ ” system into two parts, i.e., the 1- $\mu\text{m}$  cavity and the 1.5- $\mu\text{m}$  cavity. In the 1- $\mu\text{m}$  cavity there is a polarization-dependent isolator and a fiber polarization controller (PC). The two components are employed to induce NPE. An additional 1064/1550 nm WDM is used to filter out the residual 1.5  $\mu\text{m}$  radiation from the 1- $\mu\text{m}$  cavity. The output of the 1- $\mu\text{m}$  cavity is performed by the 10% port of a 10:90 fiber coupler. The 1.5- $\mu\text{m}$  cavity also comprises a polarization-dependent isolator and a PC. A 1064/1550 nm WDM is used to remove the residual 1  $\mu\text{m}$  radiation from the 1.5- $\mu\text{m}$  cavity. A customized optical delay line is employed to adjust the length of the 1.5- $\mu\text{m}$  cavity. The delay line is a fiberized device which provides variable time delay by introducing tunable path length for the laser beam. The delay line plays an indispensable role in the mode-locking of the 1.5  $\mu\text{m}$  laser. As discussed above, to activate the mode-locking of the 1.5  $\mu\text{m}$  laser through XPM, the round-trip frequency of the 1.5- $\mu\text{m}$  cavity is required to be identical with that of the 1- $\mu\text{m}$  cavity. Given that it is impractical to precisely match the round-trip time of the two cavities (which operates at 1  $\mu\text{m}$  and 1.5  $\mu\text{m}$ , respectively) via directly managing the fiber lengths, we use the delay line for the fine

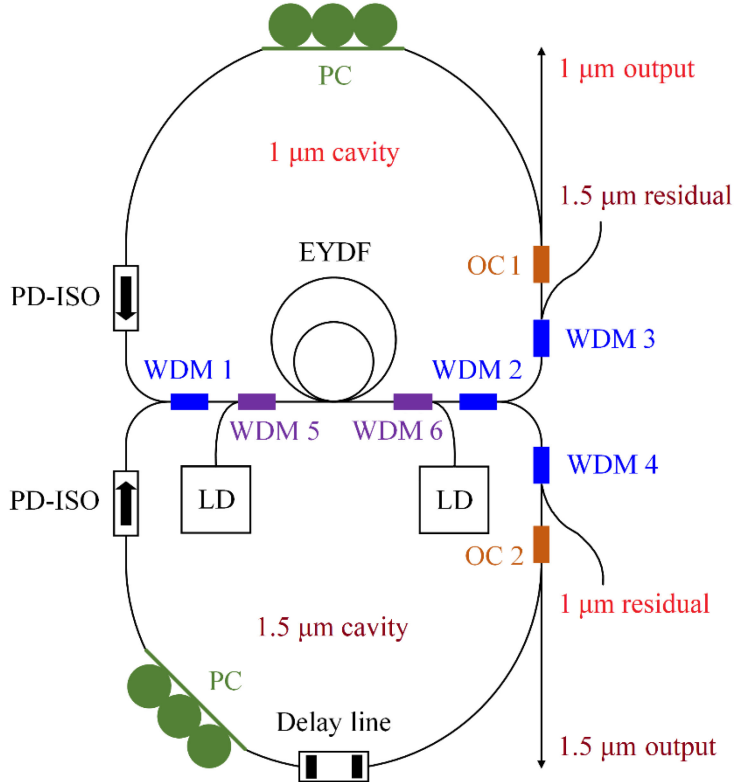


Fig. 1. Experimental setup. EYDF: Er/Yb-codoped fiber. LD: 976 nm laser diode. PC: polarization controller. PD-ISO: polarization-dependent isolator. WDM 1–4: 1064/1550 nm WDM. WDM 5, 6: 980/1064&1550 nm WDM. OC1: 1- $\mu\text{m}$  coupler. OC2: 1.5- $\mu\text{m}$  coupler.

adjustment of the 1.5- $\mu\text{m}$  cavity. The maxima delay provided by the delay line is 300 ps, which is found to be enough for realizing a highly precise match in the experimental works. The 1.5  $\mu\text{m}$  laser is sent out from the 10% port of a 10:90 coupler. The total dispersion of the 1- $\mu\text{m}$  cavity is  $\sim 0.14 \text{ ps}^2$ , whilst the total dispersion of the 1.5- $\mu\text{m}$  cavity is  $\sim -0.08 \text{ ps}^2$ . It should be noted that although the 1- $\mu\text{m}$  cavity is of an all-normal dispersion (ANDi) configuration, it is not necessary to employ a spectral filter for establishing the mode-locking, owing to the fact that NPE behaves as an equivalent filter [15].

The EY305 Er/Yb-codoped fiber plays a crucial role in the operation of the laser. The fiber has a very high absorption rate at 976 nm ( $\sim 1337 \text{ dB/m}$ ), and hence, the fiber suffers from severe “bottleneck” effect as it is pumped with the 976 nm lasers. In ordinary state an excited Er/Yb-codoped fiber emits dominantly in the 1.5  $\mu\text{m}$  band by exploiting the non-radiative energy transfer process between  $\text{Yb}^{3+}$  ions and  $\text{Er}^{3+}$  ions. As the bottleneck effect occurs, however, the emission in the 1  $\mu\text{m}$  band increases rapidly, owing to the fact that there are too many excited  $\text{Yb}^{3+}$  ions which cannot transfer their energies to  $\text{Er}^{3+}$  ions instantly, and thus, the energies will be released through the 1  $\mu\text{m}$  emission. As a result, the EY305 fiber can be used as the gain medium for both the 1  $\mu\text{m}$  and the 1.5  $\mu\text{m}$  laser. Previously a similar “figure-θ” setup for dual-band mode-locked fiber laser system has been reported by J. Zeng *et al.* [16]; in their system, however, the 1  $\mu\text{m}$  and the 1.5  $\mu\text{m}$  signals are generated in different active fibers (a Yb-doped fiber and an Er-doped fiber), and the shared section is composed of passive components. The setup demonstrated by us in this paper utilizes a single active fiber to generate the 1  $\mu\text{m}$  and the 1.5  $\mu\text{m}$  signals simultaneously, and thus, effectively reduces the cost. It should be noted that in the mechanism discussed above, to enable the bottleneck effect the Er/Yb-codoped fiber must be strongly pumped. Hence, the fiber cannot be too long for a given pump power. On the other hand, the fiber must be long enough to

provide the gain for the  $1.5 \mu\text{m}$  laser. Therefore, the length of the Er/Yb-codoped fiber should be determined carefully. In this work, the length is optimized in experiments.

The mode-locking of the  $1.5 \mu\text{m}$  laser is established via a particular mechanism that is developed in the 1990's for realizing mode-locking in fiber lasers [17]–[19]. In the mechanism, a target laser (in this case, the  $1.5 \mu\text{m}$  laser) is mode-locked through XPM induced by another mode-locked laser (in this case, the  $1 \mu\text{m}$  laser) [20]. To maximize the modulation effect of XPM, the round-trip frequency (which is determined by the cavity length) of the target laser should be identical with the repetition rate of the laser that enforces XPM on it. The pulse generated by the target laser exhibits synchronization with the pulse generated by the XPM-inducing laser. It should be noted that the mode-locking technique is entirely different from some previously reported cases regarding synchronized dual-band mode-locked fiber lasers which also utilize XPM [21], [22]. In those cases, XPM is only used to facilitate the synchronization, whilst the lasers for each spectral band have their own mode-locking mechanism (e.g., NPE, saturable absorber, etc.). In the technique discussed here, however, the mode-locking of the target laser is directly activated by XPM, and the synchronization is a subsequent effect of the mode-locking. In many aspects, the technique employed in this work is comparable with synchronous pumping that is utilized by solid-state lasers and dye lasers [23]–[25], in which a pulsed pump laser activates the mode-locking of a target laser as the round trip frequencies of the two lasers are precisely matched. On the other hand, the synchronous pumping used by the solid-state lasers and dye lasers relies on gain-modulation effect to establish the mode-locking of the target laser, instead of XPM.

### 3. Results and Discussions

In experimental works, we first raise the pump power and manipulate the PC to start the mode-locking of the  $1 \mu\text{m}$  laser. The NPE-based mode-locked fiber lasers usually suffer from low stability. This is owing to the fact that the intracavity polarization state is highly sensitive to ambient factors such as the mechanical vibration (or other motion) of fibers. In this work, on the other hand, once the mode-locking is established, its stability is sound. We have monitored the mode-locking of the  $1 \mu\text{m}$  laser for more than 30 minutes, during which we did not observe any termination or degradation of the mode-locking, as long as the positions of the PC's paddles are not changed. The high stability can be attributed to the fact that we use tapes to fix all pigtail fibers and the active fiber on the breadboard which houses the laser system for reducing the influence of ambient effects. However, such management cannot sustain long-term mode-locking operation that continues for hours or days. To further enhance the stability of the NPE-based mode-locking, we plan to employ polarization maintaining (PM) fibers to establish the cavity of the  $1 \mu\text{m}$  laser in the future works. It is known that the NPE mechanism can be realized in an all-PM-fiber cavity by special management of the splicing between PM fibers [26], [27]. Another concern over the NPE-based mode-locking is the reproducibility. It is well known that NPE effect equals to a fast saturable absorber which is difficult for self-starting. In this work, once the laser is turned off, the mode-locking cannot be reproduced by simply raising the pump power. To establish the mode-locking, it is always necessary to manipulate the PC.

After the mode-locking of the  $1 \mu\text{m}$  laser is established, the mode-locking of the  $1.5 \mu\text{m}$  laser can be started by adjusting the optical delay line to manage the length of the  $1.5 \mu\text{m}$  cavity. The XPM-induced mode-locking of the  $1.5 \mu\text{m}$  laser can be further optimized by adjusting the PC in the  $1.5 \mu\text{m}$  cavity. A steady dual-band mode-locking operation is achieved as the total pump power is increased to 703 mW, and can be sustained under the maximum pump power (1119 mW). As aforementioned, the mode-locking of the  $1.5 \mu\text{m}$  laser is achieved with an XPM-associated mechanism. It is found that the mode-locking of the  $1.5 \mu\text{m}$  laser cannot be achieved by NPE solely with the available pump power. As the cavity of the  $1 \mu\text{m}$  laser is cut off, the mode-locking of the  $1.5 \mu\text{m}$  laser cannot be started by manipulating the PC even under the maximum pump power. On the other hand, NPE indeed benefits the mode-locking of the  $1.5 \mu\text{m}$  laser, mainly in stabilizing the operation. If the polarization-dependent isolator in the  $1.5\text{-}\mu\text{m}$  cavity is replaced by a polarization-independent one, the mode-locking of the  $1.5 \mu\text{m}$  laser cannot be maintained well.

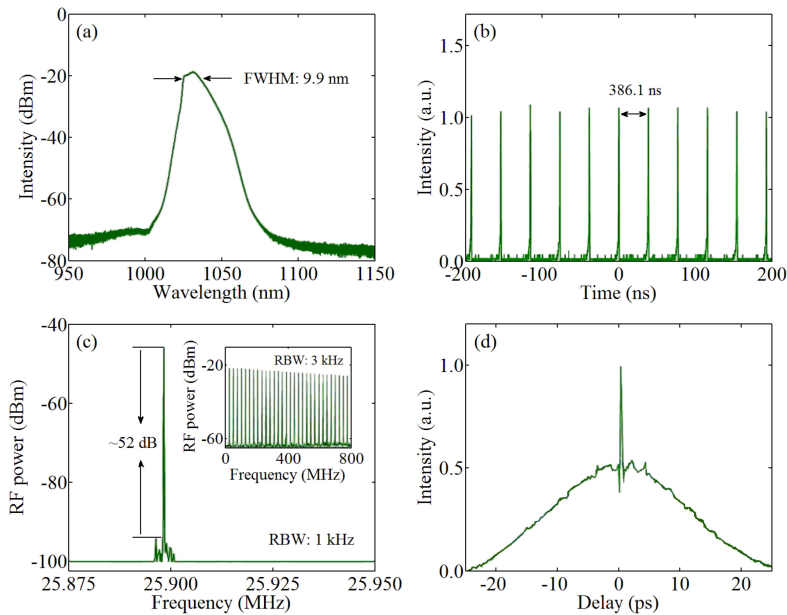


Fig. 2. (a) Output characteristics of the  $1 \mu\text{m}$  laser: (a) output spectrum under maximum pump power; (b) pulse train; (c) RF spectrum around the fundamental frequency, inset: RF spectrum in an 800-MHz span; (d) autocorrelation trace.

The output characteristics of the dual-band mode-locked fiber laser are acquired using the following equipments: optical spectrum analyzer (OSA, Yokogawa AQ6370Q), oscilloscopes (Tektronix DPO 7014C and Teledyne LeCroy SDA 820Zi-B), RF spectrum analyzer (Agilent N9320A), photodetector (Newport New Focus 1014), and autocorrelator (APE PulseCheck SM).

The output characteristics of the  $1 \mu\text{m}$  laser are presented in Fig. 2. Fig. 2(a) demonstrates the spectrum of the laser. Centered at 1031 nm, the spectrum is of a 9.9-nm FWHM. Fig. 2(b) shows the oscilloscope trace of the pulse train. The adjacent pulses are spaced by 386.1 ns. The RF spectrum of the  $1 \mu\text{m}$  laser is presented in Fig. 2(c). The repetition rate of the laser is determined as 25.89 MHz, a value that corresponds well to the 386.1-ns space between the adjacent pulses. The signal-to-noise ratio (SNR) of the fundamental frequency is determined as  $\sim 52$  dB. The RF spectrum in an 800-MHz span is shown in the inset of Fig. 2(c). No modulation on the harmonics is observed. Fig. 2(d) presents the autocorrelation trace of the  $1 \mu\text{m}$  pulse. The trace exhibits a double-scale structure with a narrow coherence peak riding on a broad pedestal, which is the representative characteristic of noise-like pulse (NLP) [28]. Given that NLP is a pulse packet consisting of numerous ultra-short pulses instead of an independent pulse [29]–[32], the pulse duration cannot be determined in a conventional way. In this work, we use the oscilloscope trace acquired with a high-speed oscilloscope (Teledyne LeCroy SDA 820Zi-B, bandwidth: 20 GHz, sample rate: 80 GS/s) and a high-speed photodetector (Newport New Focus 1014, bandwidth: 45 GHz) to estimate the temporal width of the overall NLP packet. The maximum width of the  $1 \mu\text{m}$  NLP packet is estimated to be less than 25 ps, that is, the width is beyond the detecting ability of the oscilloscope. It should be noted that in the experimental works, the laser is operating in the NLP regime throughout the tuning range of the pump power, and we could not acquire conventional pulses (e.g., dissipative soliton) by manipulating the PC. This may be attributed to the fact that the Er/Yb-codoped fiber is strongly pumped for realizing the dual-band mode-locking. The intracavity power of the laser is consequently high under such strong pumping, and thus, the pulse experiences strong nonlinear effects which lead to the formation of NLP.

The output characteristics of the  $1.5 \mu\text{m}$  laser are presented in Fig. 3. Fig. 3(a) illustrates the spectrum of the laser, which is centered at 1536 nm, and is of a 6.9-nm FWHM. The oscilloscope

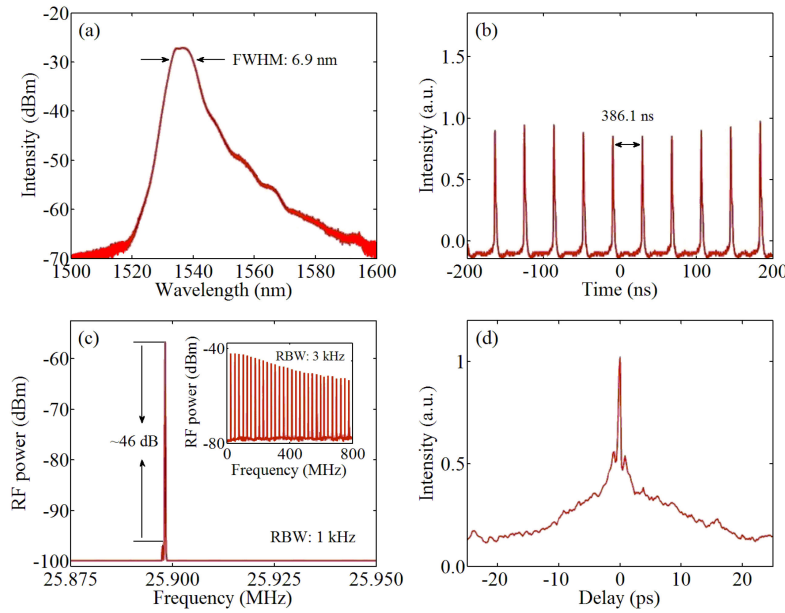


Fig. 3. Output characteristics of the  $1.5 \mu\text{m}$  laser: (a) output spectrum under maximum pump power; (b) pulse train; (c) RF spectrum around the fundamental frequency, inset: RF spectrum in an 800-MHz span; (d) autocorrelation trace.

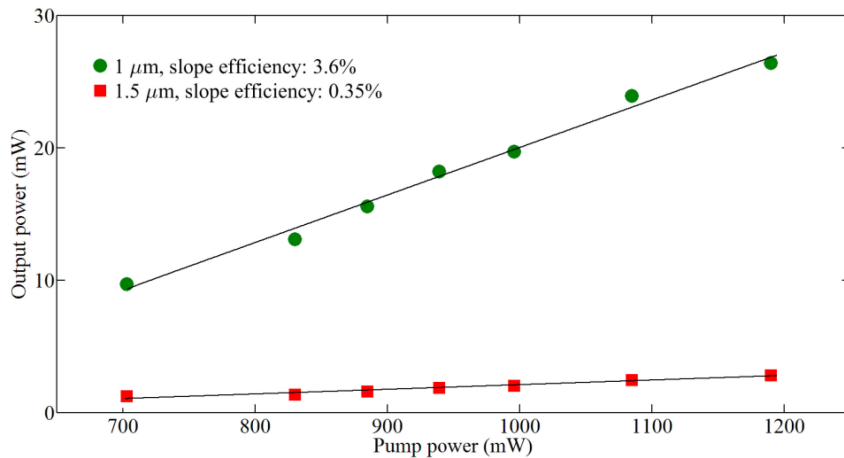


Fig. 4. Output powers as the functions of the pump power for the  $1 \mu\text{m}$  laser and the  $1.5 \mu\text{m}$  laser.

trace of the pulse train is shown in Fig. 3(b). The space between the adjacent pulses is identical to that of the  $1 \mu\text{m}$  laser (i.e., 386.1 ns). Fig. 3(c) demonstrates the RF spectrum of the  $1.5 \mu\text{m}$  laser. The fundamental frequency is of a SNR of  $\sim 46$  dB. The repetition rate of the  $1.5 \mu\text{m}$  laser (25.89 MHz) is identical to that of the  $1 \mu\text{m}$  laser, indicating that the two lasers are of synchronization. The inset of Fig. 3(c) shows the RF spectrum of the  $1.5 \mu\text{m}$  laser in an 800-MHz span. No remarkable modulation on the harmonics is observed. The autocorrelation trace of the  $1.5 \mu\text{m}$  laser is presented in Fig. 3(d). Double-scale structure is observed, indicating that the  $1.5 \mu\text{m}$  laser also operates in NLP mode. The width of the  $1.5 \mu\text{m}$  NLP packet is estimated to be less than 25 ps.

Finally, the output power of the dual-band mode-locked fiber laser is investigated. Under the maximum pump power (1119 mW), the output powers of the  $1 \mu\text{m}$  laser and the  $1.5 \mu\text{m}$  laser are respectively 27.5 mW and 2.8 mW (see Fig. 4). Taking the repetition rate (25.89 MHz) into

account, the powers correspond to a pulse energy of 1.06 nJ for the 1  $\mu\text{m}$  laser and a pulse energy of 0.11 nJ for the 1.5  $\mu\text{m}$  laser. The imbalance between the output powers/pulse energies of the two-color pulses is insignificant for some applications like difference frequency generation (DFG), and it can be easily compensated in subsequent managements of the laser beams.

## 4. Conclusion

In this paper, we experimentally demonstrate a dual-band mode-locked fiber laser operating in the 1  $\mu\text{m}$  and the 1.5  $\mu\text{m}$  band simultaneously. Thanks to the mechanism based upon XPM-induced mode-locking, the laser realizes synchronization between the 1/1.5  $\mu\text{m}$  pulses. Moreover, the “figure- $\theta$ ” architecture enables the laser to generate the two-color pulses using a single active fiber, a fact that provides the system outstanding compactness and cost-effectiveness. The laser is of attractiveness for certain applications, such as the seed laser of the pump sources for ultra-broadband supercontinuum generation.

## References

- [1] M. E. Fermann, A. Galvanauskas, G. Sucha, and D. Harter, “Fiber-lasers for ultrafast optics,” *Appl. Phys. B: Lasers Opt.*, vol. 65, pp. 259–275, 1997.
- [2] W. Q. Zhang, D. G. Lancaster, T. M. Monro, and S. A. Vahid, “Synchronised dual-wavelength mode-locking in waveguide lasers,” *Scientific Reports*, vol. 8, 2018, Art. no. 7821.
- [3] M. V. Ponarina *et al.*, “Dual-wavelength generation of picosecond pulses with 9.8 GHz repetition rate in ND: YAG waveguide laser with graphene,” *Quantum Electron.*, vol. 49, no. 4, pp. 365–370, 2019.
- [4] X. Ma *et al.*, “Single- and dual-wavelength switchable mode-locked dissipative soliton Yb-doped fiber laser based on graphene/WS2 nanocomposites modelocker and polarization controller,” *Appl. Phys. Exp.*, vol. 12, 2019, Art. no. 112006.
- [5] X. Li, S. Dai, W. Zou, J. Chen, Q. Nie, and S. Dai, “Simultaneous emission of Gaussian-like and parabolic-like pulse waveforms in an erbium-doped dual-wavelength fiber laser,” *Scientific Reports*, vol. 7, 2017, Art. no. 9414.
- [6] F. Ganikhanov, S. Carrasco, X. S. Xie, M. Katz, W. Seitz, and D. Kopf, “Broadly tunable dual-wavelength light source for coherent anti-Stokes raman scattering microscopy,” *Opt. Lett.*, vol. 31, no. 9, pp. 1292–1294, 2006.
- [7] M. Rusu, R. Herda, and O. G. Okhotnikov, “Passively synchronized erbium (1550-nm) and ytterbium (1040-nm) mode-locked fiber lasers sharing a cavity,” *Opt. Lett.*, vol. 29, no. 19, pp. 2246–2248, 2004.
- [8] M. Zhang, E. J. Kelleher, A. S. Pozharov, E. D. Obraztsova, S. V. Popov, and J. R. Taylor, “Passive synchronization of all-fiber lasers through a common saturable absorber,” *Opt. Lett.*, vol. 36, no. 20, pp. 3984–3986, 2011.
- [9] C. Guo, S. Ruan, H. Lin, L. Wen, D. Ouyang, and J. Yu, “Ultra-wideband supercontinuum light source based on dual-band fiber laser,” U.S. Patent 20160190764A1, 2016.
- [10] R. K. Shelton *et al.*, “Subfemtosecond timing jitter between two independent, actively synchronized, mode-locked lasers,” *Opt. Lett.*, vol. 27, no. 5, pp. 312–314, 2002.
- [11] T. R. Schibli *et al.*, “Attosecond active synchronization of passively mode-locked lasers by balanced cross correlation,” *Opt. Lett.*, vol. 28, no. 11, pp. 947–949, 2003.
- [12] D. Yoshitomi, Y. Kobayashi, H. Takada, M. Kakehata, and K. Torizuka, “100- attosecond timing jitter between two-color mode-locked lasers by active–passive hybrid synchronization,” *Opt. Lett.*, vol. 30, no. 11, pp. 1408–1410, 2005.
- [13] C. Fürst, A. Leitenstorfer, and A. Laubereau, “Mechanism for self-synchronization of femtosecond pulses in a two-color Ti:Sapphire laser,” *IEEE J. Sel. Topics Quantum Electron.*, vol. 2, no. 3, pp. 473–479, Sep. 1996.
- [14] D. Wu *et al.*, “Passive synchronization of 1.06- and 1.53-  $\mu\text{m}$  fiber lasers Q-switched by a common graphene SA,” *IEEE Photon. Technol. Lett.*, vol. 26, no. 14, pp. 1474–1477, Jul. 2014.
- [15] L. Zhao, D. Tang, X. Wu, and H. Zhang, “Dissipative soliton generation in Yb-fiber laser with an invisible intracavity bandpass filter,” *Opt. Lett.*, vol. 35, no. 16, pp. 2756–2758, 2010.
- [16] J. Zeng, B. Li, Q. Hao, M. Yan, K. Huang, and H. Zeng, “Passively synchronized dual-color mode-locked fiber lasers based on nonlinear amplifying loop mirrors,” *Opt. Lett.*, vol. 44, no. 20, pp. 5061–5064, 2019.
- [17] E. J. Greer and K. Smith, “All-optical FM mode-locking of fiber laser,” *Electron. Lett.*, vol. 28, no. 18, pp. 1741–1743, 1992.
- [18] M. L. Stock and L.-M. Yang, “Synchronous mode locking using pump-induced phase modulation,” *Opt. Lett.*, vol. 18, no. 18, pp. 1529–1531, 1993.
- [19] D. S. Peter, G. Onishchukov, W. Hodel, and H. P. Weber, “570 fs pulses from a Pr<sup>3+</sup>-doped fiber laser modelocked by pump pulse induced cross-phase modulation,” *Electron. Lett.*, vol. 30, no. 19, pp. 1595–1596, 1994.
- [20] M. Wegmüller, W. Hodel, and H. P. Weber, “Fiber laser mode-locking by pump pulse induced cross-phase modulation: A numerical analysis,” *Opt. Commun.*, vol. 115, pp. 498–504, 1995.
- [21] K. Huang, X. Gu, H. Pan, E. Wu, and H. Zeng, “Synchronized fiber lasers for efficient coincidence single-photon frequency upconversion,” *IEEE J. Sel. Topics Quantum Electron.*, vol. 18, no. 2, pp. 562–566, Mar./Apr. 2012.
- [22] B. Tsai, S. Wu, C. Hu, W. Hsiang, and Y. Lai, “Subfemtosecond hybrid synchronization between ultrafast yb and er fiber laser systems by controlling the relative injection timing,” *Opt. Lett.*, vol. 38, no. 17, pp. 3456–3459, 2013.

- [23] L. F. Mollenauer, N. D. Vieira, and L. Szeto, "Mode locking by synchronous pumping using a gain medium with microsecond decay times," *Opt. Lett.*, vol. 7, no. 9, pp. 414–416, 1982.
- [24] C. J. Flood, G. Giuliani, and H. M. van Driel, "Observation of mode locking in a synchronously pumped Nd:YAG laser," *Opt. Lett.*, vol. 15, no. 4, pp. 218–220, 1990.
- [25] S. Kelly, G. H. C. New, and D. Wood, "Mode-locking dynamics of synchronously-pumped colour-centre lasers," *Appl. Phys. B*, vol. 47, pp. 349–357, 1988.
- [26] Z. Wu, Q. Wei, P. Huang, S. Fu, D. Liu, and T. Huang, "Nonlinear polarization evolution mode-locked YDFL based on all-PM fiber cavity," *IEEE Photon. J.*, vol. 12, no. 2, Apr. 2020, Art. no. 1501807.
- [27] J. Szczepanek, T. M. Kardaś, C. Radzewicz, and Y. Stepanenko, "Ultrafast laser mode-locked using nonlinear polarization evolution in polarization maintaining fibers," *Opt. Lett.*, vol. 42, no. 3, pp. 575–578, 2017.
- [28] M. Horowitz, Y. Barad, and Y. Silberberg, "Noiselike pulses with a broadband spectrum generated from an erbium-doped fiber laser," *Opt. Lett.*, vol. 22, no. 11, pp. 799–801, 1997.
- [29] D. Tang, L. Zhao, and B. Zhao, "Soliton collapse and bunched noise-like pulse generation in a passively mode-locked fiber ring laser," *Opt. Exp.*, vol. 13, no. 7, pp. 2289–2294, 2005.
- [30] L. M. Zhao and D. Y. Tang, "Generation of 15-nJ bunched noise-like pulses with 93-nm bandwidth in an erbium-doped fiber ring laser," *Appl. Phys. B: Lasers Opt.*, vol. 83, no. 4, pp. 553–557, 2006.
- [31] L. M. Zhao, D. Y. Tang, J. Wu, X. Q. Fu, and S. C. Wen, "Noise-like pulse in a gain-guided soliton fiber laser," *Opt. Exp.*, vol. 15, no. 5, pp. 2145–2150, 2007.
- [32] S. Kobtsev, S. Kukarin, S. Smirnov, S. Turitsyn, and A. Latkin, "Generation of double-scale femto/pico-second optical lumps in mode-locked fiber lasers," *Opt. Exp.*, vol. 17, no. 23, pp. 20707–20713, 2009.